Madridge
Journal of Nanotechnology & Nanoscience

Research Article

Open Access

Characterizing the Gas adsorption-dependent Dielectric Constant for Silicalite Nanoparticles at Microwave Frequencies by a Coaxial Cable Fabry-Pérot Interferometric Sensing Method

Shixuan Zeng[1], Adam Trontz[1], Zishu Cao[1], Hai Xiao[2] and **Junhang Dong[1]***

[1]Department of Chemical and Environmental Engineering, University of Cincinnati, Cincinnati, OH 45221, USA
[2]Electrical and Computer Engineering Department, Clemson University, Clemson, SC 29634, USA

Article Info

***Corresponding author:**
Junhang Dong
Department of Chemical and Environmental Engineering
University of Cincinnati
Cincinnati, OH 45221
USA
E-mail: Junhang.dong@uc.edu

Received: May 2, 2018
Accepted: May 17, 2018
Published: May 22, 2018

Citation: Zeng S, Trontz A, Cao Z, Xiao H, Dong J. Characterizing the Gas adsorption-dependent Dielectric Constant for Silicalite Nanoparticles at Microwave Frequencies by a Coaxial Cable Fabry-Pérot Interferometric Sensing Method. *Madridge J Nanotechnol Nanosci.* 2018; 3(1): 98-105.
doi: 10.18689/mjnn-1000119

Published by Madridge Publishers

Abstract

The understandings of dielectric and optical properties and their dependencies on molecular adsorption are critical to many important applications of zeolite materials. This article presents the characterization of dielectric constant for the pure-silica MFI-type zeolite (silicalite) nanoparticles in a high frequency range of 0.002 – 6 GHz by a new metal ceramic coaxial cable Fabry-Pérot interferometer (MCCC-FPI) sensor platform. The overall dielectric constant of the silicalite nanoparticle packed-bed and the intrinsic dielectric constant of the silicalite crystals have been measured by the new MCCC-FPI sensing method under conditions of isobutane adsorption. The MCCC-FPI sensor platform demonstrated in this study may provide a convenient and reliable means for characterizing the molecular adsorption-dependent dielectric properties for a variety of useful nanoporous materials such zeolites, metal-organic frameworks, and microporous solid oxide catalysts.

Keywords: Zeolite; Dielectric constant; Adsorption-dependence; Coaxial cable; Fabry-Pérot interferometer.

Introduction

Zeolites are nanoporous aluminosilicate crystals that possess useful dielectric and optical properties for a number of important applications, for instances, as photonic materials, low-k electronic elements, ionic conductors, molecular probes, and photo- and microwave catalysts, etc [1-6]. Many optical properties of zeolites, such as the refractive index, IR spectrum, UV/vis light absorbance, and Raman shift, vary instantly upon adsorbing molecular species (guest) onto or desorbing adsorbate molecules from the surfaces of the zeolitic cavities. Thus, zeolite materials has been utilized as probing materials to establish various optical sensors for chemical detections and analyses. The refractive index of zeolites is well-known to vary sensitively with molecular adsorption into the crystalline structure. The dependence of refractive index on the adsorbate concentration has been utilized to develop optical means for studying molecular diffusion in zeolites and establishing zeolite film-coated fiber optic sensors [7,8]. Because of the fundamental relationship between refractive index n and dielectric constant ε_r of non-magnetic materials as expressed by equation (1), ε_r values of zeolite crystals must be also dependent of the adsorbate concentration.

$$\varepsilon_r^c = \varepsilon_r + i\varepsilon_r^i = n_c^2 = (n + i\kappa)^2 \quad (1)$$

where ε_r^c and n_c are complex relative permittivity and complex refractive index, respectively; ε_r and ε_r^i are real and imaginary relative permittivity, respectively; and *n* and *κ* are the real and imaginary (i.e. extinction coefficient) parts of the refractive index, respectively. Although numerous research works have been reported in the literature with focuses largely on the synthesis and application of zeolites as dielectric or electronic materials, the measurement of the molecular adsorption-dependent dielectric constants of zeolites has remained quite limited especially in the microwave frequency range.

The understanding of zeolites' dielectric behaviors and their relationship with molecular adsorption in the zeolitic pores of nanometer or sub-nanometer scales has been hindered by the lack of simple and reliable measurement technologies. Currently, the widely used capacitance measurement approach applies to low frequency ranges while the conventional techniques for measurements in microwave frequency ranges often involve challenging and costly device fabrication and encounter difficulties in controlling sample conditions during operation [9,10]. This paper reports the measurement of dielectric constant for pure silica MFI-type zeolite (i.e. silicalite) nanoparticles in the microwave frequency range of 1 – 6 GHz by a new metal-ceramic coaxial cable Fabry-Pérot interferometer (MCCC-FPI) sensor approach, which was recently developed by the authors [9,10]. The MFI-type zeolite has been specifically selected for this study because it is a very versatile group of materials that has so far attracted the most extensive research efforts in exploration of new applications as catalysts, low-k electronic components, ion conductors, and photonic and microwave substrates, etc. The measurement of the silicalite ε_r under gas adsorption state by the MCCC-FPI method is demonstrated using isobutane (*i*-C_4H_{10}) as the sample gas in this work because of the availability of its extensive thermo physical properties and specified Langmuir adsorption equation of state [11,12].

Silicalite nanoparticles and *i*-C_4H_{10} adsorption

The MFI-type zeolite has a topological structure shown in Figure 1, where two interconnected channel systems exist in the crystal, namely the nearly-cylindrical straight channels (0.56nm x 0.53nm aperture) in *b*-direction and the zigzag channels (0.55nm x 0.51nm aperture) running in the *a*-*c* plane. The unit cell is of orthorhombic structure (*Pnma*) with dimensions of *a* = 20.1Å, *b* = 19.7Å, and *c* = 13.1Å.The pure-silica MFI-type zeolite (silicalite) nanoparticles were synthesized by the in situ hydrothermal crystallization method. This synthesis method was originally developed by Vroon [13] and a modified synthesis procedure was also described in our previous publication [14]. The chemicals used in zeolite synthesis included fumed silica powders (99.8%, Aldrich), sodium hydroxide (99.998%, pellet, Aldrich), deionized (DI) water, and tetrapropylammonium hydroxide (TPAOH, 1M, Aldrich).The dry air, helium (>99.999%), and isobutane (>99.5%) gases were obtained from Wright Brothers, Inc. (Cincinnati, OH, USA).

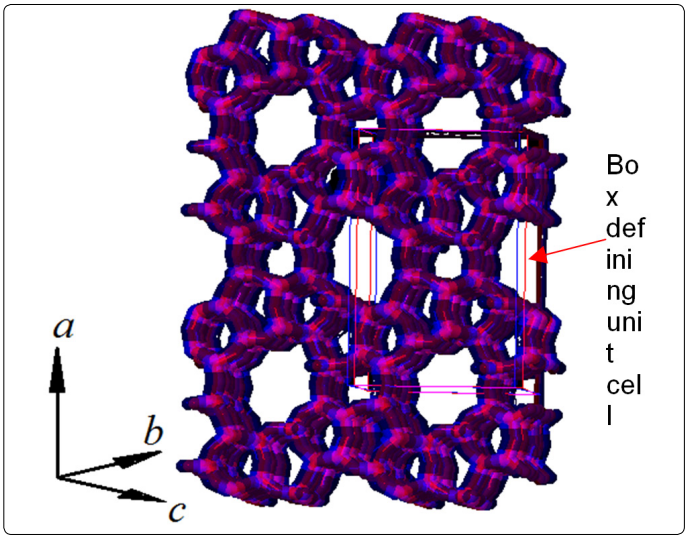

Figure 1. Schematic showing the topological structure of the MFI-type zeolite crystal.

The precursor for zeolite synthesis was a clear solution with molar ratio of 0.33(SiO_2): 0.1(TPAOH): 0.035(NaOH): 5.56(H_2O), where the TPAOH was used as structure directing agent (SDA) for the MFI-typezeolite. This synthesis solution was prepared by dissolving the fumed silica and NaOH pellets in 1M TPAOH solution at 80°C with the addition of DI water. The precursor was incubated statically at room temperature for 4h. The hydrothermal crystallization process was accomplished in a Teflon-lined autoclave at temperature of 120°C for a duration of 12 h. After the hydrothermal reaction, the resultant silicalite nanoparticle slurry was filtered and washed repeatedly by DI water; and then the particles were recovered from the suspension by centrifugal segregation. The silicalite nanoparticles were dried and calcined in air at 500°C for 4 h to remove the SDA and free up the zeolitic pores. The silicalite nanoparticles were found to be in spherical shape with uniform diameter of around 100 nm as measured by a particle size analyzer (90 Plus, Brookhaven) and confirmed by high resolution scanning electron microscopic (SEM) observations. Figure 2 shows the SEM image of the zeolite particles together with the results of X-ray diffraction (XRD) and energy dispersive X-ray spectroscopy (EDS) examinations. The XRD and EDS test results verified that the zeolite particles were of pure MFI-type crystal phase and the zeolite was of pure silica in the structure.

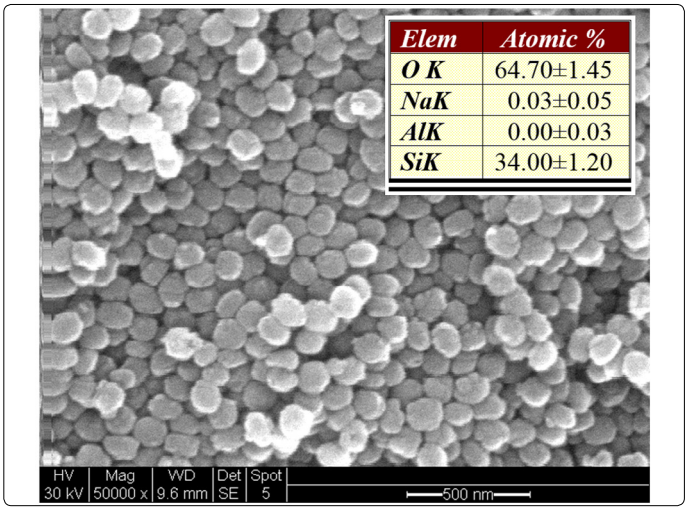

(a)

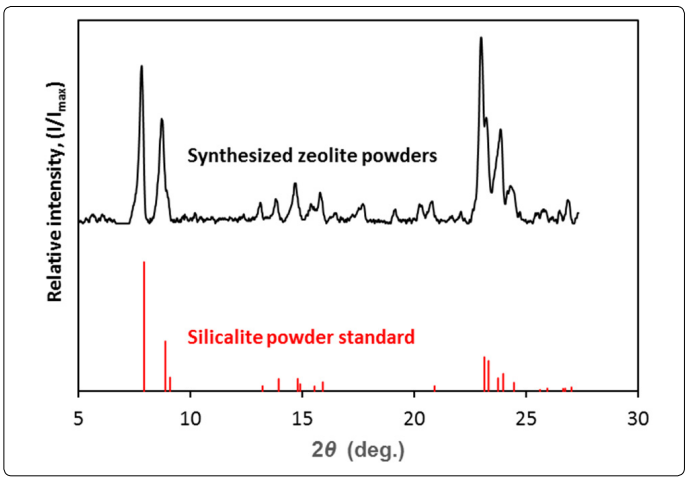

(b)

Figure 2. Results of SEM, EDS, and XRD examinations for the zeolite particles obtained by the in situ hydrothermal crystallization method: (a) SEM image with insert displaying elemental compositions obtained by the EDS analysis, and (b) XRD pattern in comparison with silicalite powder standard [15]

In our recent study, the isotherms of isobutane adsorption in silicalite were experimentally measured in a temperature range from room temperature to 120°C, as shown in Figure 3 [12]. The isobutane isotherms were found to be well-correlated by the following Langmuir equation of state,

$$q = q_{\max} \frac{K_L p_{iB}}{1 + K_L p_{iB}} \quad (2)$$

where q and q_{max} are the amount of adsorbed gas (*mmol/g*) at gas pressure p_{iB} and the maximum amount of adsorption at a given temperature; K_L is the temperature-dependent Langmuir constant.

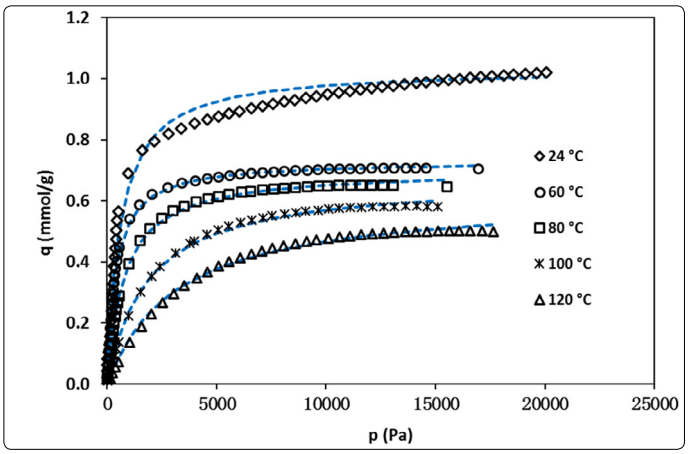

Figure 3. Experimental isotherms of isobutane in silicalite and correlations by the Langmuir equation (dashed lines).

The isobutane concentration in the zeolite at equilibrium state under isobutane partial pressure of p_{iB} is $C_\infty = q \cdot \rho_z$ where ρ_z is the silicalite density (=1.76 g/cm^3) [16]. At room temperature (22.3°C), the Langmuir equation constants $q_{\max}$ and K_L, are found to be 1.049×10^{-3} mol/g and 1.743×10^{-3} Pa^{-1}, respectively, based on their correlated temperature dependencies. The Langmuir equation fully specified by these constants has been used in this work to quantify the isobutane concentration in the zeolite crystls, i.e.molecular loading defined by "number of molecules per unit cell", under the given p_{iB} at measurement temperature (22.3°C). The room temperature (22.5°C) dielectric constant of isobutane gas at 3.25×10^5 Pa is 1.0092 [11].

MCCC-FPI sensor fabrication

Coaxial cables are radio frequency wave guides composed of three coaxially aligned components, including a metal wire inner conductor at the center, a tubular metal shield outer conductor, and a layer of dielectric material (i.e. electrical insulator) filling the annular space between the inner and outer conductors. The MCCC is a specialty coaxial cable recently developed in our laboratory. The MCCC possess extraordinary thermal and chemical stabilities as well as mechanical strength that are desirable for constructing microwave sensors [9]. The microwave FPI can be established by introducing two dielectric perturbations into the electric insulation layer in a distance of "*d*" to act as weak reflectors in the coaxial transmission line. In the MCCC-FPI sensor of this work, the two dielectric perturbations are the interfaces at the two ends of a cavity created inline of the MCCC insulator where two materials of different ε_r values meet [10]. The basic structure of the zeolite particle-packed MCCC-FPI sensor is schematically depicted in Figure 4, which is a modified version of our recently reported coaxial cable FPI liquid sensor. The MCCC-FPI sensor was constituted by four main components, including a stainless steel (SS) tube outer conductor, an SS wire inner conductor, two pieces of dense alumina tube for insulation, and a test chamber in between the two ends of the alumina tubes for housing the sample bed of solid particles and flowing sample gas of interest.

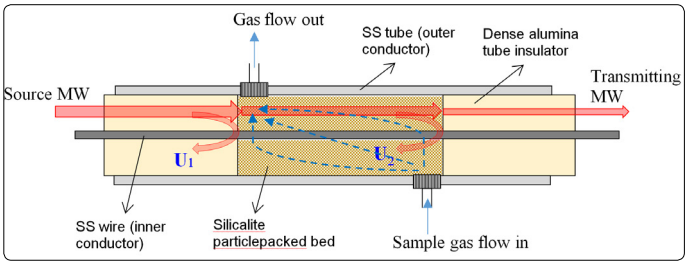

Figure 4. Schematic showing the structure of the silicalite nanoparticle packed MCCC-FPI sensor.

In this study, the SS tube had an outer diameter (OD) of 6.35 mm andan inner diameter (ID) of 4.58 mm (Grade 316, ASTM A213/A269); the SS wire had a diameter of 1.62 mm (Grade 316L, ASTM A555/A580); and the alumina tube had an OD of 4.57 mm and ID of 1.63 mm (99.5% α-Al_2O_3, 95% density). The SS tube and wire and the alumina tubes were obtained commercially from McMaster Carr (Cleveland, Ohio, USA) and Ceramic Solutions Inc. (Hawthorne, California, USA), respectively. The SS tube had two holes drilled at the two ends of the sample chamber section for connections to vacuum pump or the gas supply. In assembling the MCCC-FPI, one of the alumina insulators was firstly fixed on to the SS wire by alumina-based ceramic adhesive and then inserted into the SS tube to position the alumina tube end at the gas line inlet. The silicalite powders were introduced from the open end of the SS tube under the assistance of vacuum suction. A long alumina tube was used to compact the packed

bed of zeolite powders while the vacuum suction continued to increase the packing density. This procedure of vacuum suction and compacting by tube pressing was repeated for several times until a silicalite bed was formed to cover the two holes for tubing connections. Finally, another 10-cm long alumina tube insulator was inserted into the SS tube from the open end, which was subsequently attached onto the inner and outer conductors using the ceramic adhesives.

The lengths of the SS tube (30 cm) and the two pieces of alumina tube (both 10 cm) were carefully measured. Thus the length of the zeolite-packed sample chamber (d) can be readily obtained from the segments of the alumina tubes remaining outside the SS tube. The sample chamber was about 12 cm long, which was defined by the positions of the two holes on the SS tube for gas flow. The position of the alumina tube remaining outside of the SS tube was physically locked by alumina-based ceramic adhesives to allow for restoring the exact position of the alumina tube end after the packed particles were removed. Based on the ε_r values of vacuum (1.0) or (dry air ~1.0003), the vacuumed or air-filled sample chamber can be used to accurately determine chamber length d either by scanning the microwave interferogram or more conveniently by recording the time domain spectrum of the FPI [10]. After determining the accurate chamber length d, the volume fractions of the zeolite particles (φ_z) and inter-particle voids (i.e. porosity) of the zeolite packed-bed (φ_v) are obtained from the amount of the packed zeolite (m_z) as following,

$$\varphi_z = 1 - \varphi_v = \frac{m_z/\rho_z}{\pi(r_{tube}^2 - r_{wire}^2)d} \quad (3)$$

Principle of ε_r measurement and experimental procedure

The MCCC-FPI depicted in Figure 4 was connected to the microwave transmission line. The source microwave propagating along the coaxial cable generates two reflections (U_1 and U_2) at the two reflectors, i.e. the interfaces at the two ends of the sample chamber. The two reflections, U_1 and U_2, interfere and the interference waveform is expressed by the following equation [10],

$$U = 2j \cdot \Gamma(f) e^{-\alpha z} e^{-j2\pi f \frac{2d_0\sqrt{\varepsilon_{r,1}} + d\sqrt{\varepsilon_r}}{c}} \sin\left(2\pi f \frac{d\sqrt{\varepsilon_r}}{c}\right) \quad (4)$$

where $\Gamma(f)$ is the frequency-dependent reflection coefficient of the reflectors; z signifies the propagation direction; α is the transmission attenuation coefficient; d_0 is the propagation distance prior to the first reflector; ε_r is the dielectric constant of the packed-bed between the reflectors; c is the speed of light in vacuum; and d is the sample chamber length. Equation (4) indicates that, for a given FPI with known component materials, structural parameters, and operation temperature, the resonant frequencies of the reflected microwave interferogram depends solely on the optical length ($d\sqrt{\varepsilon_r}$) of the sample bed. Thus, the reflected interferogram can be recorded to monitor changes in the optical length of the sample-filled cavity ($d\sqrt{\varepsilon_r}$). By tracking the microwave spectroscopic resonant peaks in the frequency domain, the dielectric constant of the sample-bed in the chamber is readily obtained as following

$$\varepsilon_{r,sb} = \left(\frac{Nc}{2df_N}\right)^2 \quad (5)$$

where $\varepsilon_{r,sb}$ is the overall dielectric constant of the packed-bed of particles in the sample chamber; N is the number of resonant peak in the frequency range of operation; f_N is the resonant frequency of Nth peak. For the measurement of a packed-bed containing solid particles and inter-particle spaces, the $\varepsilon_{r,sb}$ can be well represented by a linear dependence of particle packing density, i.e. volume fraction of solid ($\varphi_{r,z}$) [17]

$$\varepsilon_{r,sb} = \varepsilon_{r,z}\varphi_{r,z} + \varepsilon_{r,g}(1-\varphi_z) = \varepsilon_{r,g} + \varphi_{r,z}(\varepsilon_{r,z} - \varepsilon_{r,g}) \quad (6)$$

where $\varepsilon_{r,z}$ and $\varepsilon_{r,g}$ are the dielectric constants of the solid particles and gas in the inter-particle voids in the sample chamber.

The experimental measurement system is schematically illustrated in Figure 5. One end of the MCCC-FPI cable was connected to a vector network analyzer (N9923A RF VNA; Keysight Technologies, Eaglewood, CO, USA) through a communication coaxial cable and the other end was sealed with a short-circuit-terminator. The FPI sensor was hosted in a temperature programable forced covection oven and the sample chamber was connected to the gas supply on one end and the exiting port was connected to a 3-way valve, which could switch between the normal ventilation and the vacuum pump. The sample gas, i.e. isobutane carried in helium flow, was regulated by mass flow controllers to vary the isobutane partial pressure p_{iB}, which was verified by a bubble flow meter accurately measuring the helium and isobutane flow rates before mixing. The the microwave spectrum was swept by the VNA at a step of 6 MHz over a bandwidth range from 2 MHz to 6 GHz. The microwave signal reflected from the FPI sensing chamber was recorded and processed by a PC workstation connected to the VNA. The time for scanning the entire spectrum from 2 MHz to 6 GHz was about 1s. The microwave signal was first Fourier-transformed and then gated on the two reflection peaks to eliminate noises such as the reflections from the connections betweent the MCCC and communication cable and the short-circuit end [18].

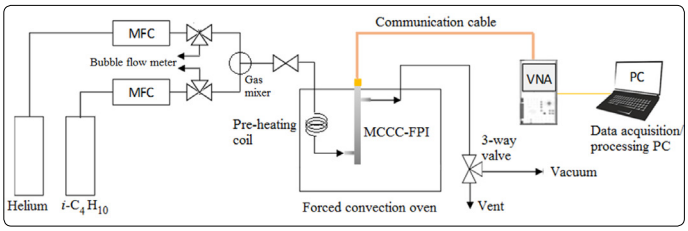

Figure 5. Schematic diagram of the MCCC-FPI measurement system.

The silicalite particles and the FPI sample chamber were thoroughly degassed before measuring the microwave interference from the FPI under isobutane adsorption. In the degassing process, the MCCC-FPI sensor was heated to 150°C followed by helium purging at 10 cm^3 (STP)/min for 1 hour and then the sample chamber underwent evacuation by the vacuum pump at < 100 Pa for 2 hours. This helium-purging and vacuuming degassing process was repeated to ensure

that the silicalite particles were free of pre-adsorbed molecules in the zeolitic channels. The oven was then turned off and the sensor was naturally cooled to room under continued vacuuming. The interferogram of the silicalite-packed FPI sample chamber was then scanned under vacuum and in pure helium flow, respectively. The interferograms obtained under these two conditions had no appreciable differences in resonant peak frequencies because the ε_r of the non-adsorbing single atomic helium gas (1.000067) is very close to that of vacuum [19]. Thus, for convenience of operation, isobutane was carried in helium at a total flow rate of 10 cm^3 (STP)/minfor studying the effect of its adsorption on the silicalite dielectric constant. For more strict measurement of the gas-adsorption dependence of zeolite dielectric contestant, a large tank of sample gas with pre-set pressure may be used to supply the environmental gas without using the carrier gas [12]. The interferogram under each equilibrium p_{iB} (given by volume fraction of the gas flow at ambient pressure) was recorded after the reflection spectrum was fully stabilized.

Results and Discussion

In this study, the dielectric constant measurements were all conducted at room temperature (22.5°C±0.3°C). The measurement of ε_r for dense particles of pure silica was performed using packed particles of ground quartz wool (SiO_2, Elementar, Langenselbold, Germany) for validation of the above described new MCCC-FPI method. The silica material was found to have no appreciable impurity by EDS examinations. The amount of silica powder packed in the FPI sample chamber was 0.5298+0.0010g. The interferogram shown in Figure 6 (a) was recorded for the MCCC-FPI with the packed silica particles. Figure 6 (b) displays the time domain spectrum of the FPI with no silica particles loaded, i.e. the FPI chamber was simply filled with dry air (ε_r =1.0003). The density and dielectric constant of pure silica are well known to be 2.65 g/cm^3 and 3.20 – 3.76 (from static to 25GHz), respectively [20,21].

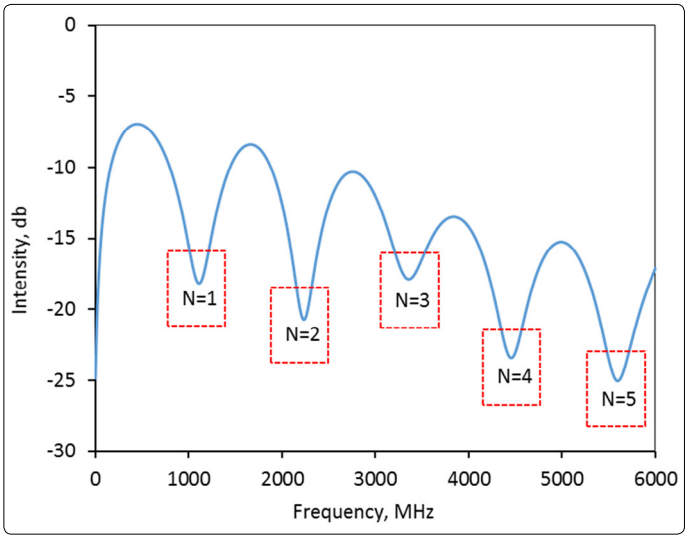

(a)

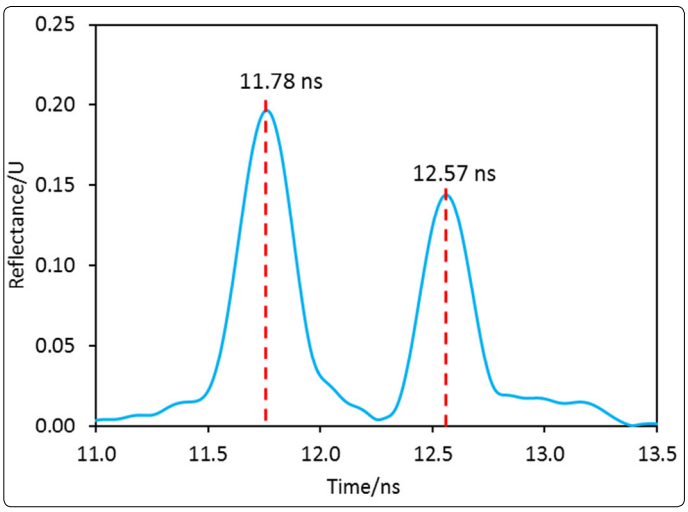

(b)

Figure 6. Results of measurements for the silica-packed MCCC-FPI: (a) The frequency domain interferogram of the silica powder-packed MCCC-FPI and (b) the time domain spectrum of the air-filled MCCC-FPI.

In Figure 6 (a), there are 5 resonant peaks in the scanned frequency range and the specific frequencies are used to compute the $\varepsilon_{r,sb}$ (i.e. overall dielectric constant of the packed bed composed of particles and air-filled voids) by equation (5) based on the *d* value determined by the delay time of the second reflection in Figure 6 (b), i.e. Δt = 12.57 – 11.78 = 0.79 ns. The chamber (particle packed-bed) length *d* (=Δt × c/2) was found to be 11.88 cm. The intrinsic dielectric constant of dense silica ($\varepsilon_{r,silica}$) was then obtained by equation (6). The experimentally measured $\varepsilon_{r,sb}$ and the subsequently calculated $\varepsilon_{r,silica}$ are listed in Table 1. Pure silica is one of the most extensively characterized dielectric materials and its $\varepsilon_{r,silica}$ values in the open literature are confirmed with high reliability. The $\varepsilon_{r,silica}$ values measured in this study were in excellent agreement with the literature values that validated the MCCC-FPI sensor platform for measuring packed-bed of dielectric solid particles and the intrinsic dense particle dielectric constants.

Table 1. The $\varepsilon_{r,sb}$ and $\varepsilon_{r,silica}$ obtained by the FPI measurement.

N	f_N/GHz	$\varepsilon_{r,sb}$	$\varepsilon_{r,silica}$
1	1.11	1.30	3.58
2	2.21	1.30	3.59
3	3.34	1.28	3.43
4	4.45	1.29	3.47
5	5.59	1.28	3.35

The sample chamber was then thoroughly cleaned and loaded with 1.4642g±0.010g of silicalite nano-particles. The chamber length was re-measured by recording the time domain spectrum after removing the zeolite particles. Figure 7 shows the frequency domain spectrum of the silicalite-packed MCCC-FPI and the time domain spectrum of the empty (air-filled) MCCC-FPI. The *d* value of the sample chamber packed with silicalite was found to be 11.42 cm, which was consistent with the chamber length measured for the packed-bed of silica (11.88 cm). The very small difference in *d* was caused by the deviation in volume control and compacting of the packed-bed. This difference though would

not affect the calculation of the dielectric constants because the actually determined lengths were always used when processing data for the specific packed-beds.

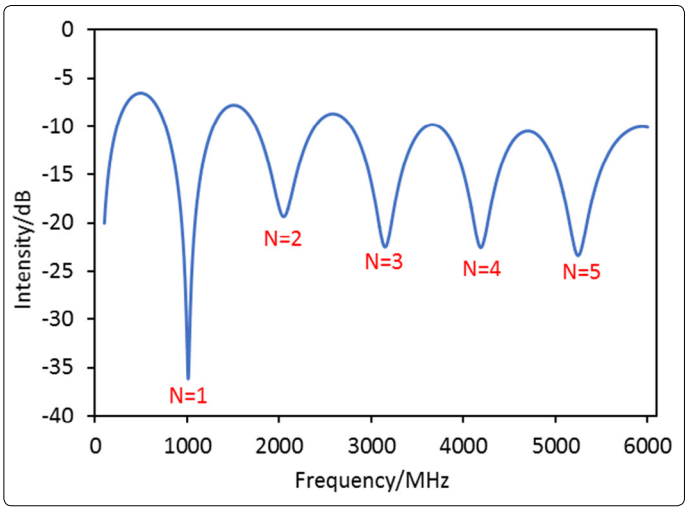

(a)

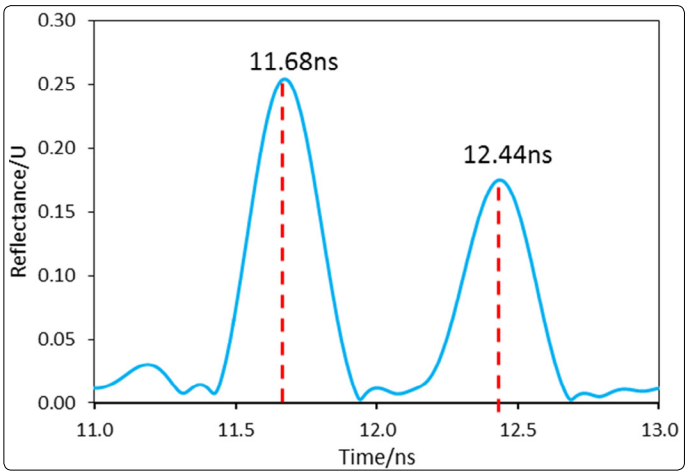

(b)

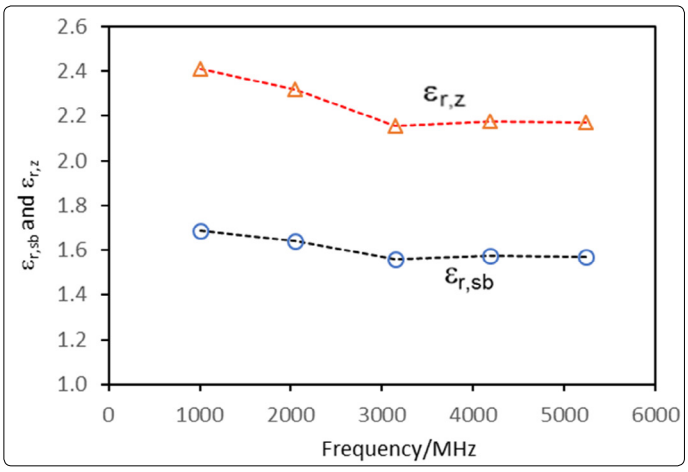

(c)

Figure 7. Results of measurement for the silicalite nanoparticle-packed MCCC-FPI: (a) the frequency domain interferogram, (b) the time domain spectrum of the air-filled chamber, and (c) the dielectric constants of the silicalite packed-bed and the silicalite crystals.

In measurement of $\varepsilon_{r,sb}$ for the silicalite packed-bed with isobutane adsorption, a step of 0.43 MHz was used for scanning the frequency domain spectra under various p_{iB} in the gas flow. This small step for spectrum scanning was used to increase the resolution for monitoring the resonant frequency shift upon gas adsorption into the zeolitic pores. However, the smaller step of frequency scanning required longer time for recording a spectrum over the entire range of 0.002 to 6 GHz by the current instrument in our lab. Therefore, the scanning frequency range was limited to 2.3 – 4.0 GHz that covered the 3rd resonant peak to shorten the measurement time. The time needed for scanning the spectrum over the range of 2.3 – 4.0 GHz was 2 s. After the isobutane volumetric or molar fraction (y_{iB}) in the gas flow of ambient pressure, i.e. $p_{iB} = y_{iB} \cdot p_{amb}$ (where ambient pressure $p_{amb} = 1.013 \times 10^5\ Pa$), was switched to a different value, the reflection intensity of a fixed single wavelength (3325.14 MHz) was continuously monitored until itwas fully stabilized to ensure that equilibrium state of gas adsorption was reached. The spectrum covering the 3rd peak range was then scanned and recorded for determining the zeolite packed-bed $\varepsilon_{r,sb}$ and the intrinsic $\varepsilon_{r,z}$ of the zeolite crystals under gas adsorption. The experimentally monitored shift of the 3rd resonant peak with increasing the equilibrium isobutane pressure (p_{iB}) in the gas flow is presented in Figure 8 (a).

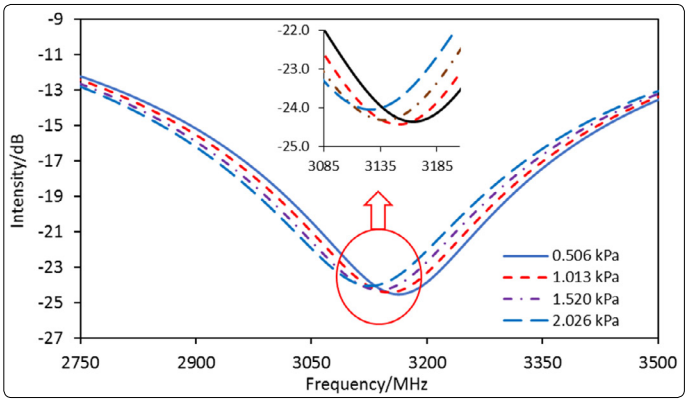

(a)

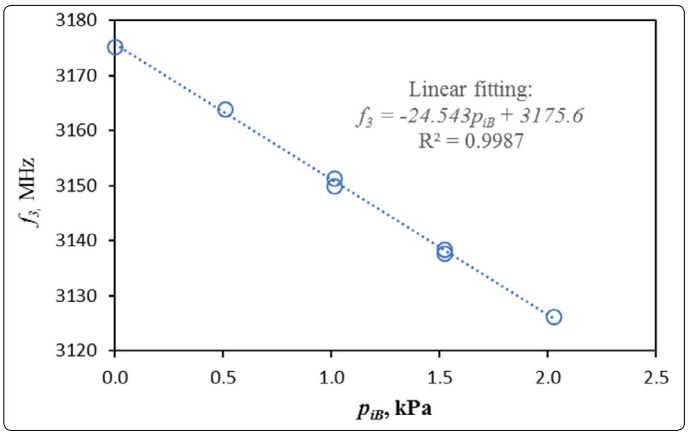

(b)

Figure 8. Shifts of the 3rd resonant peak as a function of p_{iB} for the silicalite-packed MCCC-FPI: (a) spectral shift and (b) f_3 shift.

As shown in Figure 8 (b), f_3 exhibits a linear dependence on p_{iB} in the tested range of low pressure with a slope of -24.54 MHz/kPa (isobutane). It is worth noting that the VNA had a resolution of 1 Hz per step of frequency scanning that could make the current MCCC-FPI capable of detecting a p_{iB}

change of less than 10^{-3} Pa (or 0.01 ppm in isobutane concentration at ambient pressure). This is a very high sensitivity that only allows accurate measurement of the adsorption-dependent $\varepsilon_{r,z}$ but also offers the potential as a gas sensor for trace detections.

The dielectric constants of the silicalite nanoparticle-packed bed $\varepsilon_{r,sb}$ and the zeolite crystals $\varepsilon_{r,z}$ were calculated from the 3rd resonant peak frequencies displayed in Figure 8(b). The resultant dielectric constants are presented as functions of the gas phase isobutane partial pressure p_{iB} in Figure 9, where $\varepsilon_{r,z}$ is also shown as a function of the isobutane molecular load per unit cell (n_{mlc}/*cell*). The values of (n_{mlc}/*cell*) were calculated by the specified Langmuir equation under the given equilibrium isobutane partial pressures. The dielectric constant of the silicalite crystals measured in this study was in excellent agreement with the literature values, which range from 1.8 to 2.5 depending on the measurement methods and generally decrease with increasing frequency [22, 23]. As expected from the principle of density function, increasing the gas phase pressure of the strongly adsorbing isobutane increased the amount of isobutane molecular loading inside the zeolitic pores that increased the dielectric constants of the silicalite packed-bed and the silicalite crystals. However, in Figure 9 (b), the intercepts from extrapolation of the "$\varepsilon_{r,z}$~p_{iB}" and "$\varepsilon_{r,z}$~($\frac{n_{mlc}}{cell}$)" linear correlations, which represent the $\varepsilon_{r,z}$ under no isobutane adsorption (or zero load), had a notable discrepancy. This inconsistency was likely caused by the underestimated molecular load in the silicalite nanoparticles because the Langmuir equation was correlated from gas adsorption data on micron-sized silicalite crystals. The silicalite nanoparticles of this study have much greater external surface areas and microporous inter-particle spaces in the packed-bed, which could increase the actual adsorption amount. This reasoning is also supported by the fact that the value of $\varepsilon_{r,z}$ at $p_{iB} = 0\ Pa$ extrapolated from the "$\varepsilon_{r,z}$~p_{iB}" correlation in Figure 9 (b) was 2.13, which was very close to the experimentally measured value of 2.15 (in Figure 7), but significantly greater than that extrapolated from the "$\varepsilon_{r,z}$~($\frac{n_{mlc}}{cell}$)" linear correlation.

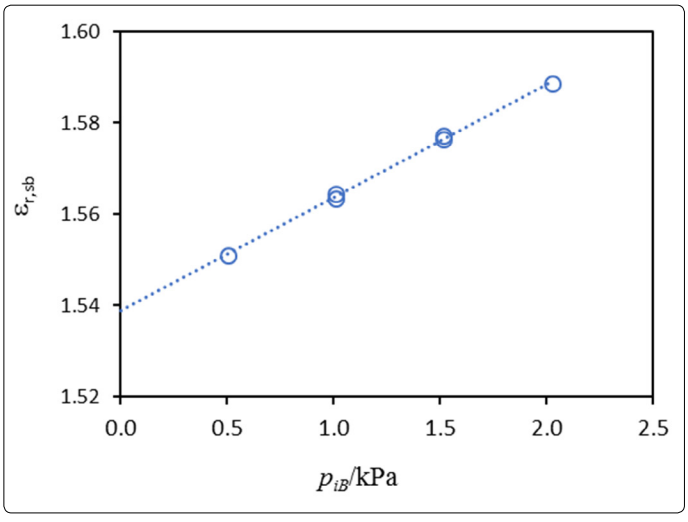

(a)

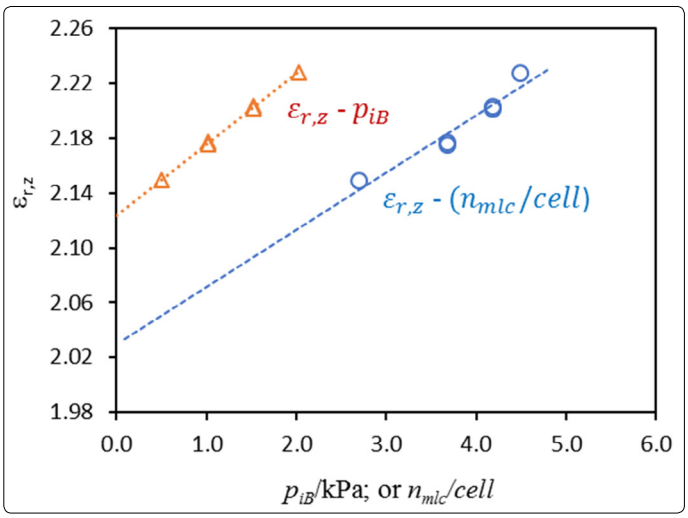

(b)

Figure 9. The $\varepsilon_{r,sb}$ and $\varepsilon_{r,z}$ determined from the frequency of the 3rd resonant peak at around 3.15 GHz: (a) $\varepsilon_{r,sb}$ as a function of gas phase p_{iB} and (b) $\varepsilon_{r,z}$ as a function of gas phase p_{iB} or as a function of molecular load per unit cell (n_{mlc}/*cell*).

Conclusion

The microwave frequency dielectric constants of the silicalite nanoparticles and their packed-bed have been measured as a function of the gas phase isobutane partial pressure using a novel MCCC-FPI sensor platform. The dielectric constant of the silicalite without adsorbing gases has been found to decrease from 2.41 to 2.17 as frequency increases from 1.01 to 5.24 GHz that is in excellent consistence with literature findings. It has been further revealed that the dielectric constant of the silicalite crystals increases with increasing the isobutane adsorption in the zeolitic pores (i.e. under higher isobutane gas pressure). In addition, the dielectric constant of the packed-bed of silicalite particles is of practical interest because the zeolite particles are commonly utilized in the form of packed columns, coated films or granulated pellets. The MCCC-FPI sensor method demonstrated in the present study may provide convenient and reliable means for characterizing the molecular adsorption-dependent dielectric properties for a variety of useful nanoporous materials such zeolites, metal-organic frameworks, and porous amorphous ceramics.

Acknowledgement

This research was financially supported by the USA Department of Energy, National Energy Technology Laboratories under grant number DE-FE0022993.

References

1. Wang Z, Wang H, Mitra A, Huang L, Yan Y. Pure-Silica Zeolite Low-k Dielectric Thin Films. *Adv. Mater.* 2001; 13(10): 746-49. doi: 10.1002/1521-4095(200105)13:10<746::AID-ADMA746>3.0.CO;2-J

2. Tiriolo R, Rangnekar N, Zhang H, et al. Tsapatsis, Sub-Micrometer Zeolite Films on Gold-Coated Silicon Wafers with Single-Crystal-Like Dielectric Constant and Elastic Modulus. *Adv. Funct. Mater.* 2017; 27(25): 1700864-1. doi: 10.1002/adfm.201700864

3. Moos R, Rauch D, Votsmeier M, Kubinski D. Review on Radio Frequency Based Monitoring of SCR and Three Way Catalysts. *Top Catal*. 2016; 59(10-12): 961-69.

4. Tang X, Provenzano J, Xu Z, et al. Acidic ZSM-5 Zeolite-Coated Long Period Fiber Grating for Optical Sensing of Ammonia. *J. Mater. Chem*. 2011; 21: 181-86. Doi: 10.1039/C0JM02523B

5. Xu Z, Michos I, Cao Z, et al. Proton-Selective Ion Transport in ZSM-5 Zeolite Membrane. *J. Phys. Chem. C*. 2016; 120(46): 26386-92. doi: 10.1021/acs.jpcc.6b09383

6. Jaymand M. Conductive polymers/zeolite (nano) composites under-exploited materials. *RSC Adv*. 2014; 4: 33935-54. doi: 10.1039/C4RA03067B

7. Schemmert U, Kärger J, Krause C, Rakoczy RA. Monitoring the Evolution of Intracrystalline Concentration. *Europhys. Lett*. 1999; 46(2): 204-10.

8. Zhang J, Luo M, Xiao H, Dong J. An Interferometric Study on the Adsorption-Dependent Refractive Index of Silicalite Thin Films Grown on Optical Fibers. *Chem. Mater*. 2006; 18(1): 4-6. doi: 10.1021/cm0525353

9. Trontz A, Cheng B, Zeng S, Xiao H, Dong J. Development of Metal-Ceramic Coaxial Cable Fabry-Pérot Interferometric Sensors for High Temperature Monitoring. *Sensors*. 2015; 15(10): 24914-25. doi: 10.3390/s151024914

10. Zeng S, Trontz A, Zhu W, Xiao H, Dong J. A Metal-Ceramic Coaxial Cable Fabry-Pérot Microwave Interferometer for Monitoring Fluid Dielectric Constant. *Sensors and Actuators: A Phys*. 2017; 257: 1-7. doi: 10.1016/j.sna.2017.02.004

11. Goodwin RD, Haynes WM. Thermophysical Properties of Isobutane from 114 to 700 K at Pressure to 70 MPa. *National Bureau of Standard Technical Note 1051*, U.S. Government Printing Office, Washington DC, USA, 1982.

12. Yang R, Xu Z, Zeng S, Jing W, Trontz A, Dong J. A Fiber Optic Interferometric Sensor Platform for Determining Gas Diffusivity in Zeolite Films. *Sensors*. 2018; 18: 1090-108. doi: 10.3390/s18041090

13. Vroon ZAEP. Synthesis and transport properties of thin ceramic supported zeolite (MFI) membranes, Ph.D. Dissertation,University of Twente, The Netherlands, 1995.

14. Tang Z, Kim SJ, Gu X, Dong J. Microwave Synthesis of MFI-Type Zeolite Membranes by Seeded Secondary Growth without the Use of Organic Structure Directing Agents. *Micropor. Mesopor. Mater*. 2009; 118(1-3): 224-31. doi: 10.1016/j.micromeso.2008.08.029

15. Baerlocher C, McCusker LB, Olson DH. Atlas of Zeolite Framework Types." 6th Ed., The Structure Commission of the international Zeolite Association, Elsevier, New York, USA, 2007.

16. Flanigen EM, Bennett JM, Grose RW, Cohen JP, Patton RL. Silicalite, a new hydrophobic crystalline silica molecular sieve. *Nature*. 1978; 271: 512-16. doi: 10.1038/271512a0

17. Si JJ, Ono H, Uchida K, Nozaki S, Morisaki H. Correlation between the dielectric constant and porosity of nanoporous silica thin films deposited by the gas evaporation technique. *Appl. Phys. Lett*. 2001; 79: 3140. doi: 10.1063/1.1415042

18. Huang J, Lan X, Zhu W, Cheng B, Fan J. Interferogram Reconstruction of Cascaded Coaxial Cable Fabry-Perot Interferometers for Distributed Sensing Application. *IEEE Sensors J*. 2016; 16: 4495-500. doi: 0.1109/JSEN.2016.2530839

19. Atanasoff JV. The Dielectric Constant of Helium. *Phys. Rev*. 1930; 36(7): 1232. doi: 10.1103/PhysRev.36.1232

20. Haynes WM. *CRC handbook of chemistry and physics*. CRC press, New York, USA, 2014.

21. Robertson J. High dielectric constant oxides. *Europ. Phys. J. Appl. Phys*. 2004; 28: 265-91. doi: 10.1051/epjap:2004206

22. Sun M, Maichen W, Pophale R, et al. Dielectric constant measurement of zeolite powders by time-domain reflectometry. *Micropo. Mesopor. Mater*. 2009; 123: 10-14. doi: 10.1016/j.micromeso.2009.03.013

23. Baklanov M, Green M, Maex K(Ed.). Dielectric Films for Advanced Microelectronics. John Willy & Sons, Ltd. Hoboken, NJ, USA, 2006.